Is it possible to extract reflection travel times from mobile receivers in a marine environment?

Nick Dorogy, Center for Wave Phenomena, Colorado School of Mines

QUESTION

The goal of this project is to model marine data acquisition from receivers floating in the water column using seismic interferometry. To accomplish this, we use random, ambient seismic sources distributed in the sea floor and receivers that are moving ir "drifting" below the surface. The primary objective is to determine if the correct travel times can be collected in this scenario. This concept can also be extended beyond the marine environment with remote sensing seismology of small planetary bodies. Although the work done for this project does not directly include imaging of the subsurface, the eventual goal is to perform travel time tomography with mobile receivers. This is relevant to imaging because it could enable an entirely new data acquisition geometry.

HYPOTHESIS

I believe that it is possible to collect accurate travel time data from floating receivers but the quality is directly dependent on an appropriate source distribution, coverage, and timing. Based on prior work, I anticipate issues consistently identifying the correct travel times because of poor signal-to-noise ratio (SNR) in the local cross correlation. Although not tested as a part of this project, I also believe that local cross-correlation results could be significantly effected by complex geologies.

PROJECT

Context

In the marine environment, ambient seismic interferometry data is commonly collected with ocean-bottom nodes (OBN) or receiver arrays located on the surface. OBN acquisition is done in the low-noise environment that is preferable for boosting SNR in interferometry. However, lifespan, and thus improved time-averaged SNR, are restricted by on-board power supply. Data processing and analysis must also be postponed until the nodes are retrieved thereby further extending mission time frame. Surface floating receivers can draw continuous power with solar arrays and relay data immediately via satellite connection, but the high frequency noise environment near the ocean surface can make the retrieval of accurate interferometric travel times challenging. Moreover, floating receivers do not benefit from the fixed positioning of nodes provided in OBN acquisition so drifting must be accounted for during data processing. To achieve a high spatial coverage with broad illumination in either OBN or surface acquisition geometries, a significant number of nodes will have to be deployed.

Receivers suspended in the water column may provide a compromise between the two aforementioned acquisition geometries. Proximity to the surface (within 100's of meters) allows for continuous power and communications via tethered buoys, but also provides isolation from the disruptive noise at the surface. If we allow these receivers to float while recording, we can also boost spatial coverage and illumination with the same small number of nodes. Subsequent analysis in this report determines the feasibility of this acquisition geometry by comparing the travel times acquired with an active shot survey to those recovered by the seismic interferometry technique. This project is broken into two sections: the first part focuses on angle-of-arrival (AoA) filtering with stationary receivers, while the latter focuses on the local cross-correlation technique used for receivers in motion. In each experiment, receivers A and B are suspended 250 m below the water surface and are separated by a horizontal distance of 1 km. Medium velocity in the water layer is uniformly assumed to be 1.5 km/s and the water bottom is located 1 km below the sea-surface. Random sources are distributed around the seafloor, each with varying random frequency and activation timing.

Stationary

To acquire true travel times between the receivers, we first model a controlled, active source emitted at the position of receiver A while receiver B records the arrival energies as shown in Figure 1. Each event in this shot record indicates arrival energy from a different ray path. Because we are not stationed at a boundary interface (i.e. directly at the seafloor or sea surface), we can observe both multiple and ghost arrivals from various different angles of arrival. In this study, we will target the water bottom reflection travel time between the two receivers. We can analytically compute the correct travel time with

$$t_{(A\rightarrow B,refl)} = \frac{2}{c}\sqrt{(\frac{\delta x_R}{2})^2 + (\delta z_{RS})^2} \qquad (1)$$

where c is the medium velocity, δx_R is the horizontal spacing between receivers and δz_{RS} is the distance between the water bottom and the receivers. Given the receiver geometry described previously, we find the correct water bottom reflection travel time to be 1.20 s, corresponding to the third arrival in Figure 1.

With the analytical and active source experiments as reference, we can now switch to a passive survey using the random, unknown seismic sources. To recover the travel time estimate using seismic interferometry, we need only compute the cross-correlation of the recordings at receivers A and B. The result of the cross-correlation is displayed in Figure 2. Observe that, even with prior knowledge of the desired travel time, it is

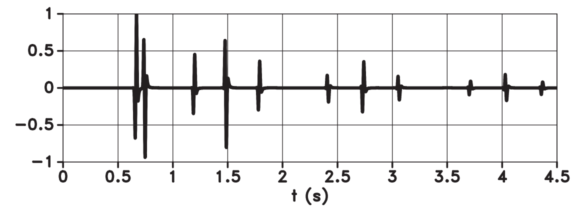

Figure 1: Data recorded by receiver B after an active shot at the location of receiver A.

not possible to locate the desired event at 1.2 s with any confidence. There are several factors that contribute to this: first, a cross-correlation between the receivers will isolate the *direct* arrival travel time, not the reflection, and second, because each receiver is suspended below the surface, the direct wave and reflected wave, as well as ghosts and multiples, will be observed as high energy events at the receivers. When we cross-correlate the data, these numerous arrivals will correlate with one another to produce cross-terms that are not physical.

In traditional active source acquisition methods, undesired direct wave energy may first be removed to preserve only the reflection energy. We must now perform a similar operation to mitigate the direct arrival, as well as the spurious ghost and multiple arrivals that are introduced by receivers suspended between boundary interfaces.

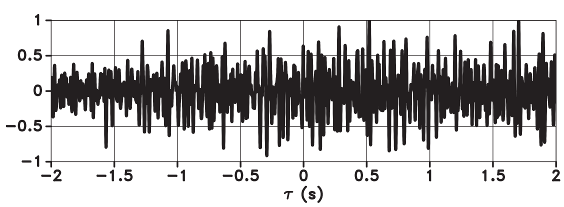

Figure 2: Cross-correlation of data at receivers A and B acquired in a passive survey. τ indicates the time lag between receivers.

To accomplish this, we take advantage of the fact that each event (i.e. ghost, multiple, etc.) will have a unique arrival angle determined by its ray path. That is, a water bottom reflection arrives at the receivers at a different angle than a ghost, for example. Thus we may implement an angle-of-arrival (AoA) filter that selects only the ray paths which we desire. For this study, we target an arrival with the ray path connecting the two receivers via a water bottom reflection. To implement this AoA filter, we will use the linear $\tau - p$ transform. This requires that we now replace the two-receiver design with two *receiver arrays.* We choose 51 individual elements for each array with 5 m of separation between individual elements.

The $\tau - p$ transform maps linear events in the time-space domain to points in the time-slowness domain, where slowness p is defined by equation 2 (Diebold and Beresford (1995)). Here, θ is the AoA on the receiver array and v is the medium velocity. If we can estimate an appropriate slowness corresponding to the ray path (and thus the angle of arrival) which we hope to keep, we can create a window around the point in the time-slowness domain to filter out other arrival angles. Then we apply the adjoint $\tau - p$ operator to return our cleaned data to the time-space domain with contributions from the direct, ghost, and multiple arrivals muted. The result of this operation should yield a receiver gather that keeps data from our desired event, while removing any spurious signal corresponding to undesired arrival energy. Therefore, we can interpret the AoA filter as a deghosting and demultipling operator that selectively preserves desired events. This in turn boosts SNR for our desired reflection response.

$$p = \frac{\sin(\theta)}{v} \tag{2}$$

$$\theta = \tan^{-1}(\delta x_R / \delta z_{RS}) \tag{3}$$

To acquire the slowness value for our filter, acoustic velocity in water is assumed to be 1.5 km/s and the arrival angle can be ascertained with know receiver positions and depths by equation 3. After finding the slowness value, we now apply the filter to each receiver array data, and once again compute the cross-correlation. The result of the $\tau - p$ filtered data is shown in Figure 3. If we compare the cleaned cross-correlation (Figure 3) with our active source acquisition (Figure 1), we observe that the reflection event occurs is highlighted at 1.2 s in both methods. However, we have yet to consider that fact that our receivers are not stationary as they float in the water column. We address this complication in the following section.

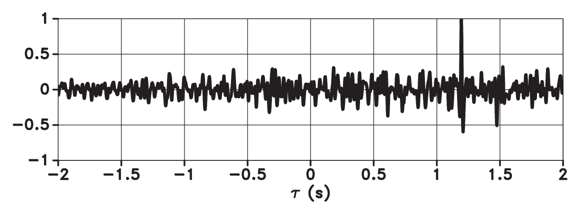

Figure 3: Cross-correlation of data at receivers A and B acquired in a passive survey after AoA filtering.

Mobile

For receivers fixed in a particular location, the aforementioned filter and cross-correlate framework performs well. But if a receiver instead "drifts" as it is suspended in water, we can now expect the cross-correlation between the two receivers to change as a function of the receiver's motion. In other words, as the receiver moves, the ray path between the receivers will change subsequently inducing a travel time that is variable with receiver and medium velocities. The cross-correlation procedure described previously fails to account for this change because the traditional method (equation 4) is integrated over the time of observation. As a consequence, variable travel times will be summed together to produce a cross-correlation that smears together many different travel times. For receivers moving significantly slower than medium velocity ($v << c$) and short acquisition times ($t << v$), this effect may be negligible. In any other case however, this smearing should not be ignored.

$$c(\tau) = \int_0^t u_A(t - {}^{\tau}/_2) u_B(t + {}^{\tau}/_2) dt \tag{4}$$

$$c(\tau) = \int_0^{\gamma} \int_0^t u_A(t - {}^{\tau}/_2) u_B(t + {}^{\tau}/_2) g(\gamma - t; \tau) dt d\gamma \tag{5}$$

Figure 4 is the AoA-filtered cross-correlation yielded when receiver B moves at a constant velocity of 10 m/s away from receiver A in a 4.5 s simulation (note that we have chosen a relatively high velocity and short observation time purely for run-time efficiency. For a more realistic acquisition, we expect $t >> v$). We can observe that the reflection travel time is no longer discernible even with an appropriately time varying AoA filter. To see the time varying cross-correlation induced by mobile receivers, we must instead use a correlation that does not require temporal integration of our data.

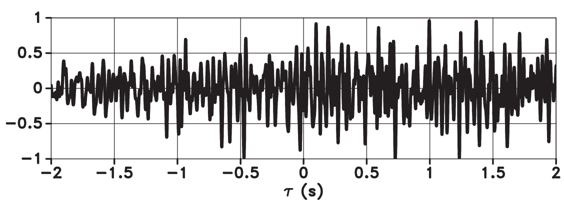

Figure 4: AoA filtered cross-correlation when receiver B moves at 10 m/s.

Hale (2006) and Hale (2013) proposes the concept of local cross-correlations or dynamic time-warping that could mitigate the observed smearing. Because dynamic time-warping is better-suited for receivers moving at high velocity, we choose to implement a local cross-correlation (equation 5). This technique first applies a Gaussian window to the data recorded by each array. Then, we must compute the cross-correlation of the windowed data. Finally, we repeat this procedure while sliding the Gaussian window over one time sample increments. Instead of producing a single, stacked cross-correlation as we have previously done, we now produce numerous cross-correlations over the entire period of observation. In other words, this technique "unstacks" the traditional cross-correlation to show how the travel time varies as a function of time. Figure 5 is a demonstration of a traditional, global cross-correlation, while Figure 6 shows the local cross-correlation method with only two example Gaussian windows applied.

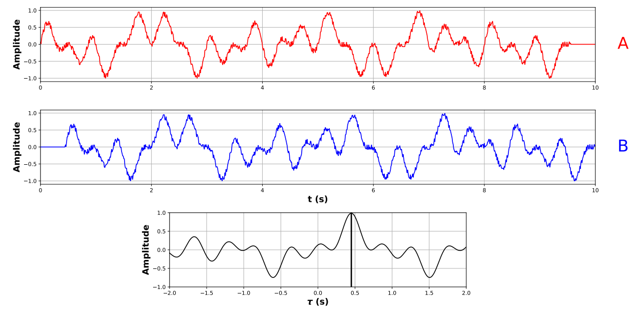

Figure 5: The signals recorded by receiver A (top) and receiver B (middle). Signal B has been delayed by 0.45 s. The resulting global cross cross-correlation from the first half of the signal is shown in the bottom left, while the result of the second half is shown in the bottom right.

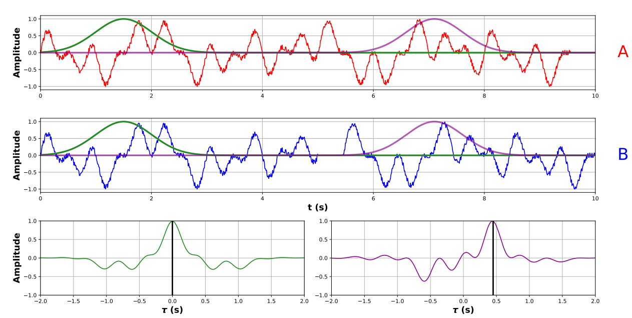

Figure 6: The signals recorded by receiver A (top) and receiver B (middle). Now, only the second half of the signal observed by B has been delayed by 0.45 s. Green and purple lines indicate Gaussian windows applied to the data. The resulting local cross cross-correlation from the first half of the signal is shown in the bottom left, while the result of the second half is shown in the bottom right. Notice that the local method was able to identify the change in the second half of the signal while preserving the 0 lag in the first half.

When both receivers are stationary (Figure 7), the local method preserves the constant travel time as we expect. However, when receiver B moves, Figure 8 allows us to view how the cross-correlation varies with observation time. The main drawback of a local-cross correlation is poorer SNR when compared with the time-stacked, traditional correlation. To improve SNR, we may deploy several receiver pairs that would allow us to ensemble average several observations over the same area.

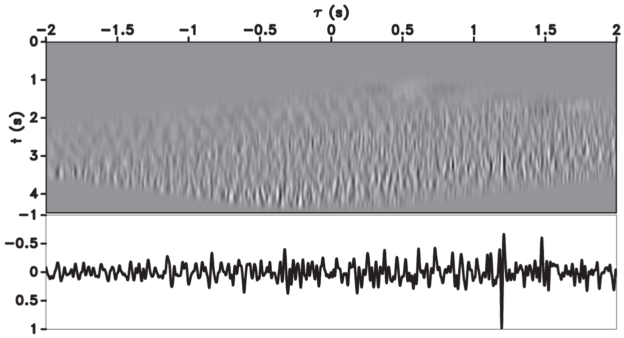

Figure 7: (Top) Result of the local cross-correlation for stationary receivers. (Bottom) The local cross-correlation stacked over time.

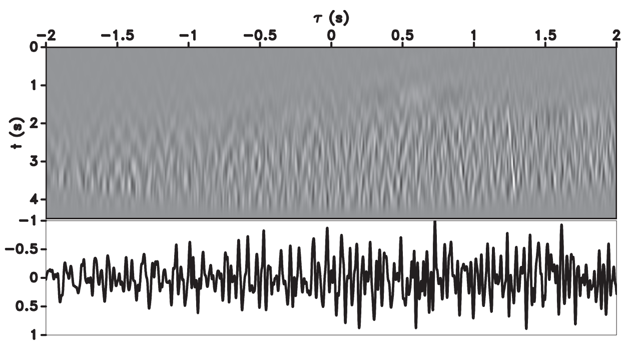

Figure 8: (Top) Result of the local cross-correlation when receiver B drifts at $10\,\mathrm{m/s}$. (Bottom) The local cross-correlation stacked over time.

CONCLUSIONS

These results suggest that seismic interferometry with receivers suspended in the water column is a realistic and feasible acquisition geometry. By introducing receiver arrays that enable us to filter for desired arrival angles, we can mitigate the contributions from unwanted arrivals. If receivers are in motion, either as they are towed or drift naturally, we use a local cross-correlation method to avoid smearing our travel times. We might also sweep our filter over a variety of angles to also image reflectors below the sea floor.

Using the proposed acquisition geometry with receivers suspended in the water column, we can combine the desired benefits of OBN and surface acquisition geometries. Suspension in the water column decouples the receivers from the noise contamination near the sea surface. However, close proximity to the surface enables us to connect to surface floating buoys that provide continuous solar power and data transmission. Although we need small receiver arrays for AoA filtering, we can allow our receivers to drift and illuminate the seafloor and deeper reflectors from numerous angles, thus avoiding the need for a large number of nodes to be deployed.

ACKNOWLEDGEMENTS

Thank you to Paul Sava for theoretical and computational contributions.

REFERENCES

Diebold, J., and G. Beresford, 1995, A review of the t-p transform, its implementation and its applications in seismic processing: Exploration Geophysics, **26**; doi: 10.1071/EG995019.

Hale, D., 2006, An efficient method for computing local cross-correlations of multi-dimensional signals: Technical report, Center for Wave Phenomena, Colorado School of Mines.

———, 2013, Dynamic warping of seismic images: Technical report, Center for Wave Phenomena, Colorado School of Mines.